RESTRAINED MODEL TESTS IN HEAD SEAS

by

E. F. SCHULZ

Civil Engineering Section
Colorado State University
Fort Collins, Colorado

Prepared for
David Taylor Model Basin
Department of the Navy
Under Contract Nonr 1610(04)
Through the
Colorado State University Research Foundation

March 1959

CER59EFS 7

RESTRAINED MODEL TESTS IN HEAD SEAS

by

E. F. SCHULZ

Civil Engineering Section
Colorado State University
Fort Collins, Colorado

Prepared for
David Taylor Model Basin
Department of the Navy
Under Contract Nonr 1610(04)
Through the
Colorado State University Research Foundation

March 1959

CER59EFS 7

ABSTRACT

This report presents the experimental forces and moments acting on a five-foot model tanker when it was towed in head seas. All the motions of the model except uniform forward translation were restrained. The model was towed in two wave lengths - approximately one-half the model length and approximately equal to model length. Three pressure gages were mounted in bottom along the keel to measure the attenuated wave pressure. The forces and moments were divided into steady-state and oscillatory forces and moments. The steady-state heaving force was independent of wave configuration and increased with increasing speed. The steady-state pitching moment was nearly independent of speed, but was strongly dependent upon wave configuration. The steady-state drag force was largely independent of wave configuration, but exhibited a complex variation with speed. The oscillatory heaving force and pitching moment increased with increasing relative wave length and speed. The oscillatory drag force was independent of wave length and increased with speed up to $Fr = 0.2$; it then decreased with further increase in speed. The greatest part of the wave attenuation occurred under the forebody. At zero speed of advance the model more effectively attenuated the shorter waves. The attenuation factor decreased with increasing speed in head seas. At higher speeds of advance the model more effectively attenuated the larger waves.

CONTENTS

TABLES

FIGURES

NOTATION

Symbol	Units	Definition
A_m	(feet)^2	Area of midship section
A_0	inches	Amplitude of undisturbed wave pressure at depth D
A_x	inches	Amplitude of Attenuated wave at distance x from bow.
A_W	(feet)^2	Waterplane area
B	feet	Beam
c	feet/sec	Wave celerity
C_B	- -	Block coefficient, $\frac{\nabla}{LBD}$
C_M	- -	Maximum section coefficient
C_W	- -	Waterplane coefficient, $\frac{A_W}{BL}$
d	feet	Depth of water
D	feet	Draft
Fr	- -	Froude number $V\sqrt{gL}$
F_x	pounds	Force in x direction
F_z	pounds	Force in z direction
f	cps	Wave Frequency
g	ft/sec^2	Acceleration of gravity 32.16 ft/sec^2
h	feet	Wave height (double amplitude)
K	- -	Subsurface pressure response factor
L	feet	Waterline length
L_{BP}	feet	Length between perpendiculars
M_ψ	inch-pounds	Pitching Moment
T_e	seconds	Period of encounter
v	feet /sec	Speed of model
χ	degrees	Angle of heading of ship relative to direction of wave travel

NOTATION - - Continued

Symbol	Unit	Definition
λ	feet	Wave length
ϑ	degrees	Wave slope
ν	radians / sec	Natural frequency
ω	radians / sec	Wave circular frequency
ω_e	radians / sec	Frequency of encounter
Δ	pounds	Displacement of Model
∇	$(\text{feet})^3$	Volume of displacement

I. INTRODUCTION

The research work described in this report was conducted for the David Taylor Model Basin, Department of the Navy, Under Contract Nonr 1610(04). The experiments were carried out in the outdoor 40-ft. x 62-ft. wave basin previously described in (1).

Experiments were carried out on a 5-foot model tanker in head seas ($\chi = 180^0$). The same model was used in previous experiments reported in (2), and was the Model "H" tanker used in the resistance tests reported by Couch and St. Denis (3). The hull sections and lines and the hull characteristics are presented in reference (2).

In some instances seaworthiness tests are conducted on model ships when some of the motions of the model are either deliberately or inadvertently restrained. In order to gain a better understanding of how to interpret the results from such model tests, the present series of experiments were initiated. During all the experiments carried out under the current contract, all of the usual motions of the model were entirely restrained while it is towed in waves and the forces and moments acting on the model are measured. A six-component force balance was constructed to provide electrical signals proportional to the forces and moments acting on the model.

In addition, instrumentation was installed to measure the wave pressure fluctuations at three points along the keel of the model and six wave probes were constructed to measure the configuration of the waves around the model. The pressure gages will yield information on attenuation of the waves by the model and where this attenuation occurs along the length of the model. The wave probe network will yield information on the reflection of the waves from the ship. The attenuation of the waves by the ship and the reflection of the waves by the ship are the major ways in which the ship affects the seaway and will, therefore, serve to provide correction coefficients to the classical assumption that the ship does not affect the seaway.

II. METHOD AND PROCEDURE

The model used was a 5-ft. tanker constructed from fiberglass-plastic laminate and reinforced with aluminum frames.

Forces and Moments

A force balance was constructed to measure the six components of force and moments acting on the restrained model while the model was being towed at different speeds and different headings in regular waves. The time history for each force and moment was recorded on a multi-channel oscillograph. Electrical signals proportional to the forces and moments are provided by Type C-19 SR-4 strain gages. The gages were used in a Wheatstone bridge circuit employing four active arms. The bridge output was amplified using a carrier-type amplifier system. A schematic drawing showing the construction of the balance is shown in Fig. 1. Figures 2 and 3 are photographs, showing the completely assembled balance and the balance with the cover removed.

The model was attached to the lower angle or model mount. The short strut protruding from the center of the cover angle engages a special fitting on the towing carriage. Through this strut the towing carriage provides both the restraint and the reference datum.

The balance was mounted in the model so that the centerline of the balance occurred in the vertical longitudinal plane of symmetry. The horizontal axis of the force balance was in the normal waterplane of the model. Lead ballast was added so that the freely floating model was at the design water line. Thus the force springs did not carry an initial load.

Pressure Gages

Three pressure gages have been mounted through the bottom of the model. The pressure gages used for this purpose were the model PT 34-3 made by the Dynamic Instrument Company at Cambridge, Mass. The transducers are differential type gages, having a flush-mounted diaphragm one inch in diameter. They are connected to a small insulated pressure reference tank mounted in the model. Normally the pressure reference tank was sealed; however, provisions were made to attach an external pressure or vacuum source and sloping water manometer so that small increments of pressure could be applied for testing and calibrating the transducers.

These gages were installed in order to obtain measurements of the attenuation of the wave by the ship. The first gage was mounted as far forward on the longitudinal centerline as possible (Sta. 1.83); the second gage was mounted on the longitudinal centerline at the midship section and the third gage has been mounted as far aft as possible (Sta. 17.375). Fig. 4 shows the model profile, the location of the gages and the cross section of the model at the location of the gages. Fig. 5 is a photograph showing the bottom of the model with the gages installed.

Influence Probe

Six influence probes have been mounted on the towing carriage for the purpose of measuring the wave configuration in the vicinity of the model. These probes employ the principle of the change in capacitance of the air space between one plate of a capacitor and the water surface (acting as the other plate of a capacitor). This type of probe does not touch the water and therefore does not disturb the water surface. The probe unit itself is a minature transistor transmitter. It is encapsulated in a small plastic box for thermal and humidity stabilization. Fig. 6 shows the probe transmitter inside the plastic box before encapsulation and Fig. 7 is a similar view after encapsulation. The top and sides of the plastic box are covered with a layer of wire screen and aluminum foil to act as electromagnetic and solar raditional reflectors. The probe capacitor plate itself is two inches square and is mounted under the transmitter circuit visible in Fig. 6.

Each probe unit transmits its information on a separate frequency band to a receiver unit located approximately 50 feet away from the carriage. Each of six receiver units picks up the signals from its assigned probe unit and provides a recordable signal to the oscillograph.

Fig. 8 shows how these probe units are placed in relation to the model. Thus these six probes provide detailed information on the deformation of the seaway caused by the presence of the model.

Tests were run in head seas ($\chi = 180^0$) at speeds of 0, 0.63, 1.27, 2.54 and 3.17 fps, corresponding to Froude numbers 0 to 0.25. Wave lengths used were 2.4 and 4.7 feet in length, corresponding to $\lambda / L = 0.48$ and 0.94. (Additional experiments in longer waves and at other angles of heading will be carried out later. The tests reported in this report were halted due to inclement weather.) Three values of wave steepness were used, $h/\lambda = 1/40$, $1/30$, and $1/20$. The tests reported herein do not include data on the deformation of the seaway because of an antenna failure during the tests.

III. EXPERIMENTAL RESULTS

The experimental data are presented in Table 1. When the model is towed at any speed without waves, forces and moments are observed. These forces and moments are caused by

1) The acceleration of the water resulting from the velocity field which develops from the flow around the hull,

2) skin friction caused by flow between water and model,

3) the wave train produced by the model,

4) the vibration of the model supported by force balance.

The model supported by the balance is a dynamic system which is set in oscillation by the acceleration when the carriage starts and sustained by carriage vibration as the model and carriage move along the track. To obtain useful information, these vibrations must occur at a much higher frequency than the frequency of encounter of the waves. Unfortunately the natural frequency of the force balance was only 2 to 3 times greater than period of encounter. Therefore, the desired force and moment histories were affected by the noise resulting from vibrations of the model on the balance. These spurious vibrations were first eliminated from the records by hand fairing of the traces.

Steady - State Forces and Moments

The forces and moments imposed on the model by its translation in calm water are identified as "steady - state forces". These forces could also be obtained from the test runs during which waves were present by noting the apparent shift of the zero of the force or moment history from the zero index obtained before the model was started or waves were present. The steady - state forces are shown as a function of Froude Number, F_r, and relative wave length λ/L and wave steepness h/λ in Fig. 9, 10, and 11. Positive heaving force, $+ F_z$, is defined as a force which would tend to lift the model from the water (see definition diagram, page v). Positive pitching moments, $+ M_\psi$, is a moment which would tend to lift the bow from the water. Positive drag force, $+ F_x$, is a force which would tend to propel the model in a forward direction.

The other force and moments (sway force, yawing moment and rolling moment) are not shown since they are not active when the model is operating in head seas.

Oscillatory Forces and Moments

The oscillatory forces and moments imposed on the model by the waves are presented in Fig. 12, 13, and 14. In order to remove the wave steepness as a variable, the forces and moments were plotted as a ratio of the range in force (double amplitude) to the wave slope, ϑ,

for heave force $\Delta F_z / \vartheta$,

for pitching moment $\Delta M_\psi / \vartheta$,

for drag force $\Delta F_x / \vartheta$.

This is not a dimensionless ratio; however, in this form the forces and moments are analogous to the dimensionless motions shown in reference 2. The forces and moments are shown as a function of period of encounter, T_e , in parameters of relative wave length, λ / L.

The period of encounter may be computed by the equation:

$$T_e = \frac{\lambda}{2.26\sqrt{\lambda} - V \cos\chi} .$$

The period of encounter was experimentally observed from the period of the wave of encounter, which is recorded by the influence probes. The values of the period of encounter shown in Table 1 were obtained from the oscillograms.

The oscillatory forces and moments were also plotted as a function of speed in Fig. 15, 16, and 17. The data were shown in this form to serve as comparison charts for the steady-state forces on Fig. 9, 10, and 11.

Wave Attenuation

The attenuation of the waves by the ship was determined by measuring the pressure history at three points along the keel. (See Fig. 4 for the locations). Since the pressure gages on the bottom of the model at some distance below the surface of the water, the pressure fluctuations

at this depth due to the waves are less than if the gages were located at the surface of the water. The wave attenuation is defined as the ratio of the amplitude of the attenuated wave pressure (along the bottom of the model), A_x, to the amplitude of the undisturbed wave pressure at the same depth below the quiescent free surface, A_0.

The amplitude of the undisturbed wave pressure, A_0, was computed using a pressure response factor, K, given by Wiegel and Johnson (4):

$$K = \frac{h_D}{h_0} = \frac{\cosh \quad 2\pi \quad d/\lambda \quad (1 - D/d)}{\cosh \quad 2\pi \quad d/\lambda}$$

where

h_D is the wave height measured at distance D below free surface

h_0 is the wave height measured at the surface

D is the depth below the free surface

d is the total depth of the water

D/d is the proportional depth

The pressure response factor was computed for these experiments using:

1. depth below the free surface D = 0.27 feet
2. depth of water, d = 5.5 feet
3. wave length, λ, values ranging from 2.5 feet to 10 feet.

The computed pressure response factor appropriate to the model conditions are shown on Fig. 18.

The wave attenuation ratio A_x/A_0 was computed from the measurement of the three pressure gages using

$$A_0 = \frac{hK}{2}$$

A_x amplitude wave pressure measured at point x.

These data were shown on Fig. 19 and 20 in parameters of speed, Fr and relative wave length λ/L. The pressure gages were located at x/L = 0.092, 0.488 and 0.877 respectively. Lines were drawn through the average values at these points and the assumed value $A_x/A_0 = 1.0$ at $x/L = 0$.

IV. DISCUSSION OF RESULTS

In most cases the data points listed in Table I have been plotted on the respective graphs using symbols which serve to identify the various parameters. The lines drawn through the data are drawn through average values of the data for the line shown. In some instances, the experimental error and limitations of the instrumentation have caused large scatter of the data points.

Steady-State Forces and Moments

The steady-state heaving force, pitching moment, and drag force are shown on Figs. 9, 10, and 11.

Heaving Force

The steady-state heaving force shown on Fig. 9 indicates consistently increasing negative values with increasing Froude Number (increasing speed). This means that the model has a tendency to settle to a lower position with increasing speed. The translation of the model causes acceleration of the water around the hull. This velocity field in the water results in the formation of a small depression around the model, explaining the negative heaving force.

With the exception of the data at Fr = .05, there is good agreement between the force measurements when no waves were present and those runs during which waves were generated. At Fr = .05 the forces were about 75 per cent greater than the no wave values; furthermore, there was a consistent tendency for the steeper 1/30 and 1/20 waves to produce the largest negative forces. There was little or no increase in the heaving force between Fr = .05 and Fr = .1 . After Fr = .1 , the force again increased with increasing speed. Except at Fr = .05 the heaving force was essentially independent of wave steepness, γ, and relative wave length , λ/L.

Pitching Moment

The steady-state pitching moment is shown on Fig. 10 . The runs when no waves were present show consistently increasing negative values indicating that the model has a diving tendency. This may be explained by the fact that the line of action of the resistance force is located below the center line of the force balance. Since the thrust was applied (through the centerline of the force balance) above the resistance, a diving pitching moment results.

When waves are added to the environment of the model, the steady-state pitching moment shows entirely different trends than when the waves were absent. When $0 < Fr < .05$, the pitching moment shows the usual increasing diving tendency. As the speed increases beyond $Fr = .05$ the pitching moment is largely independent of speed. In all cases the shorter wave lengths, $\lambda/L = 0.48$, produced positive pitching moments. This is due to the fact that the waves are attenuated by the ship and that the afterbody experiences only the more attenuated wave, thus producing a positive pitching moment.

Drag Force

The steady-state drag force is shown on Fig. 11. The trends established by the drag force in the absence of waves are well supported by nearly all the later runs with waves present. The important increase in drag at $Fr = .1$ is masked or reduced by 50 percent to 60 percent in the presence of the waves. At all other speeds the steady-state drag force is independent of both wave length and wave steepness. At $Fr = .2$ the drag increases greatly and at $Fr = .25$ the drag is three to four times greater than at any other point.

Oscillatory Forces and Moments

The oscillatory forces and moments are presented as a function of period of encounter on Fig. 12, 13, and 14, and as a function of Froude Number on Fig. 15, 16, and 17. In all cases the force or moment was shown as the range in force (double amplitude) divided by the wave slope, ϑ. This ratio was used in an attempt to eliminate wave steepness as a variable. In some cases a grouping of the data points according to steepness can be found. This is probably caused by the fact that the reflection is a function of wave steepness.

Heaving Force

The oscillatory heaving force is shown as a function of period of encounter, T_e, in parameters of relative wave length, λ/L, on Fig. 12. Highest range of the heaving force is experienced at the lowest value of the period of encounter. The data obtained in the longer wave length, $\lambda/L = .94$, indicated that the steeper waves ($h/\lambda = 1/30$) produced somewhat lower heaving forces. This trend was not present in the shorter waves.

Oscillatory heaving force is shown as a function of Froude Number, Fr, in parameters of relative wave length, λ/L, on Fig. 15. The longer waves, $\lambda/L = .94$, produced higher ranges of the heaving force.

For either wave length, higher ranges of the heaving force were found at the higher speeds. The shorter wave length, $\lambda/L = .48$, had the smallest range at zero speed of advance whereas, the longer wave length, $\lambda/L = .94$, had minimum range of heaving force at $Fr = .05$. Data for the longer waves and the highest speed, $Fr = .25$, are not available due to malfunction of the towing motor control.

Pitching Moment

The oscillatory pitching moment is shown as a function of period of encounter on Fig. 13, and as a function of Froude Number on Fig. 16. The oscillatory pitching moment data for the longer waves are not available due to the fact that the limit stops were set too low. It is known, however, that the range of oscillatory pitching moment was greater for the longer waves. The pitching-moment data for a number of the high speed runs in the shorter waves are also questionable for the same reason.

With the exception of the high speed runs (which may be questionable) the oscillatory pitching-moment data exhibit similar trends to the heaving-force data shown on Figures 12 and 15. The oscillatory pitching moment and heaving force are materially alleviated by increasing the period of encounter. In head seas this is accomplished by a reduction in speed.

Drag Force

The oscillatory drag force is shown as a function of period of encounter in parameters of relative wave length on Fig. 14. The drag force is shown as a function of Froude Number on Fig. 17. The data on Fig. 17 suggests that the range of oscillatory drag force is independent of the relative wave length and that the range of force increases in a linear relation between $0 < Fr < .20$ and then tends to decrease again at $Fr = .25$. Unfortunately the high speed run in the longer waves was not available so that no data are available to support this trend in the longer waves.

Wave Attenuation

The wave attenuation factor was computed for each run at each pressure gage. The average value for each speed was used to draw the lines shown on Figures 19 and 20. The data points are not shown on these graphs in order to avoid confusion. The values are given in Table 1. The data for the shorter wave length, $\lambda/L = .48$, are shown on Fig. 19.

The wave attenuation shows a strong dependence on speed especially for the shorter wave length. In all cases the major part of the wave attenuation occurs under the forebody of the ship. This longitudinal asymmetry accounts for the changing trends of the steady-state pitching moment observed on Fig. 10 between the no-waves and waves-present runs.

At Fr = 0 the model attenuated the shorter waves more than the longer waves. This trend was reversed when speed of advance is introduced. At Fr = .2 greater attenuation was observed for the longer waves. This is not in accordance with existing theory.

V. CONCLUSIONS

These concluding remarks are drawn from the data obtained to date reporting the experiments in head seas. The force and moment histories are divided into two parts - the steady-state and the oscillatory forces and moments.

1. The steady-state heaving force was found to be dependent upon speed and virtually independent of wave configuration. Increasing the speed caused increasingly larger negative values (settling tendency).

2. The steady-state pitching moment in waves experienced a small variation with speed and a strong dependence on wave configuration.

3. The steady-state drag force showed a complex variation with speed and was largely independent of wave configuration. The drag force showed a large increase between $.2 < Fr < .25$.

4. The oscillatory heaving force was found to increase with relative wave length and speed.

5. The oscillatory pitching moment increased with relative wave length and speed, although only qualitative values are available for the longer waves.

6. The oscillatory drag force was found to be independent of wave length and increased with speed up to $Fr = .2$. At $Fr = .2$ the drag force decreased with increasing speed.

The wave attenuation was determined from the pressure histories measured at three pressure gages mounted in the bottom of the model along the keel.

1. The forebody was more effective in attenuating the waves than the afterbody.

2. The attenuation factor decreased as the speed increased.

3. When $Fr = 0$ the model attenuated the $\lambda/L = .48$ waves to a greater degree than the $\lambda/L = .94$ waves.

4. For all other speeds of advance the model more effectively attenuated the longer waves.

The wave reflection from the model was not obtained due to failure of the instrumentation; however, some of the data indicated that the reflection coefficients are systematically higher in the shorter and steeper waves.

It would be desirable to have additional tests at $Fr = .02$ and $.07$ to better define the curvature of some of the graphs.

REFERENCES

1. Schulz, E. F. Development of a facility for testing the performance of ship hulls in oblique seas. Fort Collins, Colorado State University, Civil Engineering Department. Report No. 54EFS 10, March 1954.

2. Schulz, E. F., T. T. Williams, and R. M. Ralston, Model tests with a tanker in oblique seas. Fort Collins, Colorado State University, Civil Engineering Department. CER57EFS 2, January 1957.

3. Couch, E. B., and M. St. Denis. Comparison of power performances of Ten 600-foot single-screw tanker hulls as predicted from Model tests. Trans. SNAME. New York, Vol. 56. pp 359-394., 416-421 , Nov. 1948.

4. Wiegel, R. L., and J. W. Johnson. Elements of wave theory. Proc. First conference on Coastal Engineering, Richmond, California. 1951. pp. 5-21.

Table 1

EXPERIMENTAL DATA

Run No.	V	Fr	Te	ϑ	h	Ao	Keel Pressure Gages #1 Ax	#1 Ax/Ao	#2 Ax	#2 Ax/Ao	#3 Ax	#3 Ax/Ao	Steady State Fz	Steady State M_ψ	Steady State Fx	Oscillatory Forces and Moments ΔF_z	$\Delta F_z/\vartheta$	ΔM_ψ	$\Delta M_\psi/\vartheta$	ΔF_x	$\Delta F_x/\vartheta$
	fps		sec	deg	in	in	in	--	in	--	in	--	lb	in-lb	lb	lb	lb/deg	in-lb	in-lb/deg	lb	lb/deg
	λ/L = .48;		h/λ = 1/40;		T = .68 sec.;		λ = 2.4 ft.;				K = .48										
1	0	0	.68	4.6	.74	.18	.11	.61	.10	.56	.07	.39	0	6.0	-.01	0.7	.159	41.0	9.33	0.22	.05
2	0	0	.68	4.4	.72	.17	.11	.65	.10	.59	.06	.35	0.1	7.0	-.01	0.7	.159	41.0	9.33	0.22	.05
3	.63	.05	.58	3.5	.56	.14	.12	.86	.08	.57	.07	.50	-0.2	1.0	-.05	0.5	.143	41.0	11.72	0.50	.143
4	.64	.05	.57	4.4	.70	.17	.12	.71	.08	.47	.06	.35	-1.3	2.0	0	0.6	.139	43.0	10.00	0.66	.153
5	.64	.05	---	---	---	---	---	---	---	---	---	---	-0.8	-2.0	-.01	---	----	----	-----	----	----
6	1.25	.10	.50	4.7	.75	.18	.11	.61	.10	.56	.06	.33	-1.2	0.5	-.03	0.8	.170	48.0	10.21	0.70	.149
7	1.26	.10	.50	4.5	.72	.17	.11	.64	.08	.47	.07	.41	-1.3	1.0	-.07	1.0	.227	48.0	10.91	0.81	.189
8	1.29	.10	---	----	---	---	---	---	---	---	---	---	-1.3	5.0	-.12	---	----	----	-----	----	----
10	2.53	.20	.40	4.1	.65	.16	.09	.57	.11	.68	.08	.50	-2.6	2.0	-.02	1.5	.375	63.0	15.95	1.30	.325
12	2.51	.20	.39	4.8	.75	.18	.12	.67	.08	.44	.06	.33	-2.5	1.0	-.01	1.3	.277	65.0	13.82	1.50	.319
13	2.54	.20	.40	----	---	---	---	---	---	---	---	---	2.3	-13.0	-.03	---	----	----	-----	----	----
14	3.17	.25	.36	4.6	.74	.18	.12	.67	.14	.78	.12	.67	-3.4	2.0	-.26	2.4	.533	74.0	16.45	0.95	.211
15	3.16	.25	.36	5.3	.85	.20	.12	.60	.16	.80	.12	.60	-3.2	1.0	-.17	2.3	.450	65.0	12.74	0.85	.167
16	3.15	.25	---	---	---	---	---	---	---	---	---	---	-3.3	-17.0	-.35	---	----	----	-----	----	----
	λ/L = .48;		h/λ = 1/30;		T = .68 sec.;		λ = 2.4 ft.;				K = .48										
17	3.17	.25	.36	5.9	.95	.23	.15	.65	.14	.61	.14	.60	-3.2	0.5	-.25	2.4	.422	*	-----	0.90	.158
18	3.16	.25	.36	6.9	1.10	.26	.14	.54	.14	.54	.14	.53	-3.4	1.0	-.35	3.0	.455	*	-----	0.94	.142
19	3.17	.25	---	----	----	---	---	---	---	---	---	---	-3.3	-13.0	-.29	---	----	----	-----	----	----
20	2.53	.20	.40	5.9	.96	.23	.17	.74	.15	.65	.12	.52	-2.8	0	.04	2.3	.397	87.0	15.00	1.45	.250
21	2.51	.20	.40	6.1	.96	.23	.20	.87	.13	.57	.11	.48	-2.6	1.5	-.05	3.0	.508	*	-----	1.30	.220
22	2.54	.20	---	----	----	---	---	---	---	---	---	---	-2.3	-10.0	.02	---	----	----	-----	----	----
24	1.25	.10	.52	7.1	1.14	.27	.15	.56	.08	.30	.10	.37	-1.7	1.5	-.03	1.1	.164	65.0	9.70	0.74	.110
25	1.25	.10	.50	7.0	1.12	.27	.17	.63	.08	.30	.10	.37	-1.1	-2.0	.02	1.0	.149	58.0	8.66	0.68	.101
26	.63	.05	.58	7.2	1.14	.27	.15	.56	.10	.37	.08	.30	-1.2	-2.0	.02	---	----	56.0	8.23	0.53	.078
27	.63	.05	.58	6.8	1.08	.26	.14	.54	.08	.31	.10	.38	-1.4	1.5	0	0.6	.092	53.0	8.16	0.50	.077
28	0	0	.68	7.3	1.14	.27	.19	.70	.07	.26	.07	.25	0	9.0	-.03	0.8	.118	63.0	9.27	0.35	.052
29	0	0	.68	6.6	1.05	.25	.20	.80	.08	.32	.07	.28	0.1	8.0	-.03	0.8	.125	65.0	9.42	0.40	.063

* Force Balance against safety stop

Table 1 (Continued)

EXPERIMENTAL DATA

Run No	V	Fr	Te	ϑ	h	Ao	Keel Pressure Gages #1 Ax	#1 Ax/Ao	#2 Ax	#2 Ax/Ao	#3 Ax	#3 Ax/Ao	Steady State Fz	Steady State Mψ	Steady State Fx	Oscillatory Forces and Moments ΔFz	ΔFz/ϑ	ΔMψ	ΔMψ/ϑ	ΔFx	ΔFx/ϑ
	fps		sec	deg.	in	in	in	--	in	--	in	--	lb	in-lb	lb	lb	lb/deg	in-lb	in-lb/deg	lb	lb/deg
	λ/L = .48; h/λ = 1/20; T = .68 sec.; λ = 2.4 ft.; K = .48																				
30	0	0	.69	10.8	1.76	.42	.19	.45	.12	.29	.10	.24	-0.1	1.5	0	1.6	.157	72.0	7.06	0.51	.050
31	0	0	.68	10.8	1.75	.42	.17	.41	.13	.31	.12	.29	-0.1	-0.5	.04	1.6	.157	80.0	7.84	0.50	.049
33	.63	.05	.58	9.7	1.54	.37	.22	.60	.16	.43	.15	.41	-1.5	-2.0	-.03	1.8	.196	*	----	0.67	.073
34	1.25	.10	.50	9.8	1.56	.37	.19	.51	.13	.35	.16	.43	-1.5	-2.0	-.11	1.7	.181	*	----	1.00	.106
35	1.25	.10	.50	10.8	1.77	.43	.20	.47	.13	.30	.15	.35	-1.2	-2.0	0	1.4	.137	*	----	1.06	.104
36	2.51	.20	.40	10.2	1.62	.39	.22	.57	.19	.49	.18	.46	-2.3	-2.0	.06	3.2	.330	*	----	1.60	.165
37	2.54	.20	.39	10.1	1.64	.39	.20	.51	.19	.49	.16	.41	-2.3	-2.0	-.10	3.0	.316	*	----	1.52	.160
38	3.11	.25	.36	10.8	1.72	.41	.14	.34	.19	.46	.18	.44	-2.9	0.5	.15	4.2	.412	*	----	1.29	.126
	λ/L = .94; h/λ = 1/40; T = .96 sec.; λ = 4.7 ft.; K = .70																				
39	0	0	.96	5.5	1.74	.61	.35	.58	.22	.36	.15	.25	-0.3	-1.5	-.05	1.4	.264	*	----	0.50	.095
40	0	0	.96	5.6	1.75	.61	.35	.58	.25	.41	.17	.28	-0.2	-1.0	-.02	1.6	.302	*	----	0.50	.095
41	.63	.05	.84	5.3	1.65	.58	.38	.66	.22	.38	.23	.40	-1.1	-9.0	0	1.2	.240	*	----	0.48	.096
42	.63	.05	.85	5.5	1.74	.61	.39	.64	.22	.36	.21	.34	-0.8	-12.0	-.01	1.4	.264	*	----	0.53	.100
44	1.25	.10	.76	5.5	1.72	.60	.40	.67	.20	.33	.23	.38	-1.0	-9.0	-.11	1.6	.308	*	----	0.82	.158
45	1.27	.10	.75	5.7	1.76	.62	.39	.63	.19	.31	.23	.37	-1.3	-9.0	-.03	1.4	.259	*	----	0.85	.157
46	2.53	.20	.63	5.7	1.76	.62	.40	.65	.24	.39	.23	.37	-2.8	-9.0	.02	2.7	.500	*	----	1.63	.302
47	2.54	.20	.62	5.5	1.74	.61	.34	.56	.25	.41	.24	.39	-2.6	-6.0	0	2.8	.528	*	----	1.63	.308
	λ/L = .94; h/λ = 1/30; T = .96 sec.; λ = 4.7ft; K=.70																				
48	0	0	.96	7.5	2.37	.83	.50	.60	.25	.30	.25	.30	-0.2	-3.0	-.05	1.6	.228	*	----	0.62	.089
49	0	0	.95	4.9	2.32	.81	.59	.73	.24	.30	.25	.31	-0.1	-3.0	-.06	1.8	.261	*	----	0.65	.094
50	.63	.05	.84	7.5	2.37	.83	.55	.66	.27	.33	.26	.31	-1.4	-6.0	0	1.5	.214	*	----	0.94	.134
51	.63	.05	.85	7.7	2.40	.84	.59	.70	.27	.32	.25	.30	-1.3	-7.0	-.01	1.6	.222	*	----	0.87	.121
52	1.25	.10	.76	7.7	2.40	.84	.58	.69	.27	.32	.26	.31	-1.5	-6.0	-.02	1.8	.257	*	----	0.97	.139
53	1.25	.10	.76	7.8	2.44	.85	.61	.72	.27	.32	.26	.31	-1.4	-6.0	-.06	1.5	.206	*	----	1.06	.145
54	2.55	.20	.63	4.9	2.30	.81	.59	.73	.31	.38	.30	.37	-2.3	-4.0	0	2.4	.348	*	----	1.70	.246
55	2.57	.20	.62	7.5	2.36	.83	.65	.78	.31	.37	.29	.35	-2.8	-4.0	-.07	3.0	.428	*	----	1.69	.242

* Force Balance against safety stop.

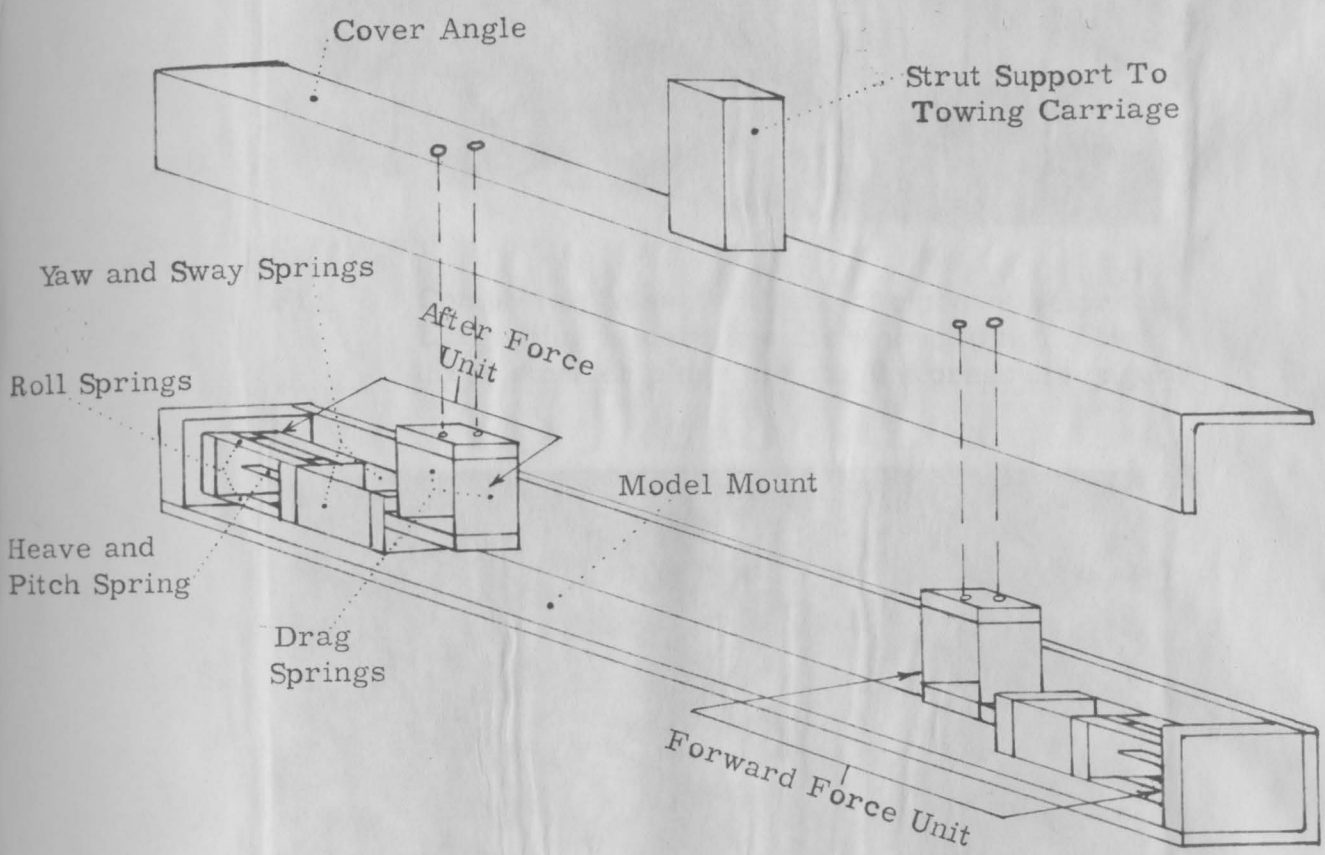

SIX COMPONENT BALANCE

Fig. 1

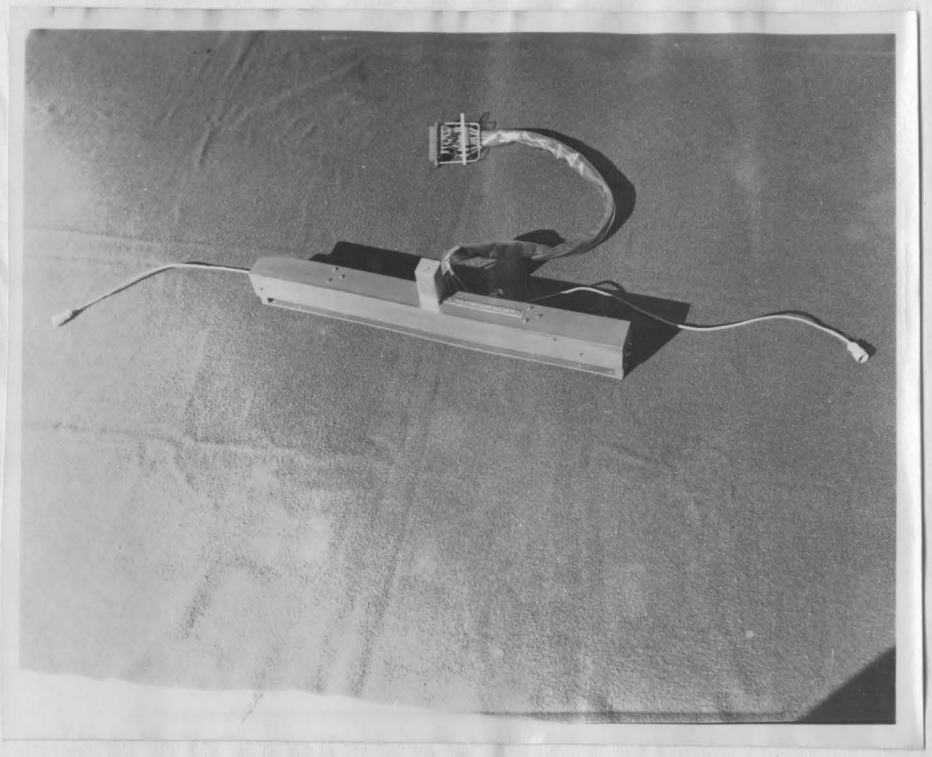

Fig. 2 Completely assembled six-component balance. Large plug is carriage disconnect plug. The three smaller plugs are for the pressure gages.

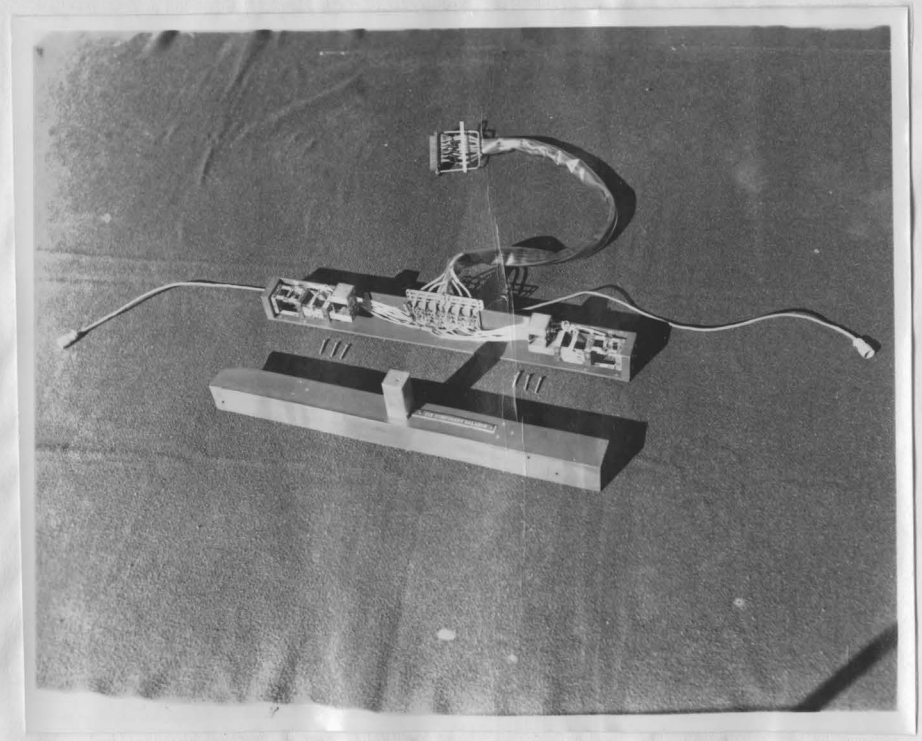

Fig. 3 Six-component balance with the cover removed, showing the forward and after force units.

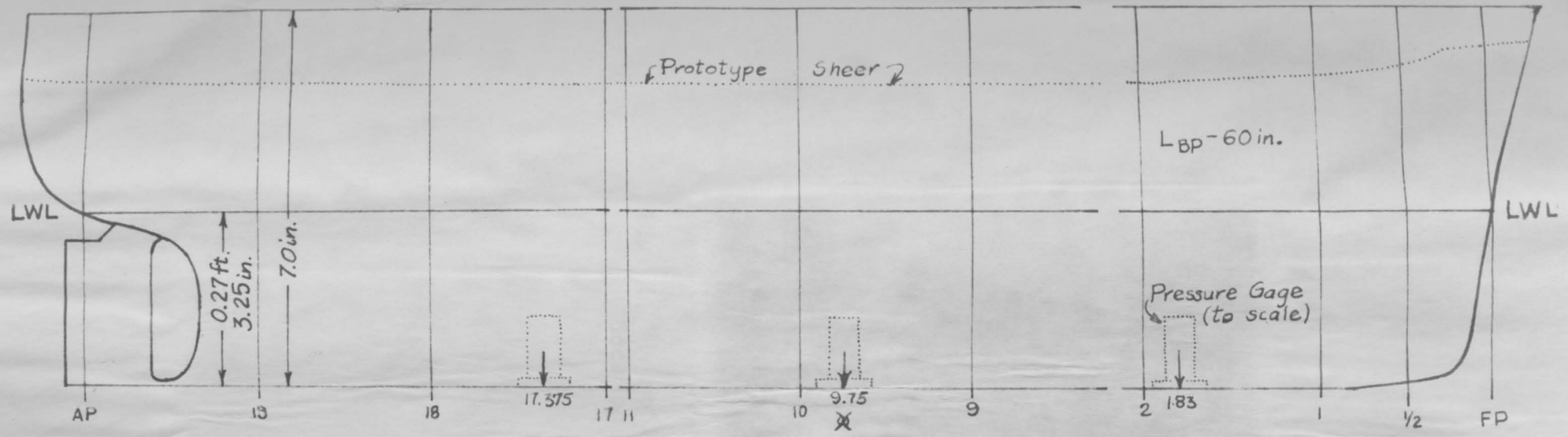

Hull Stations

MODEL PROFILE

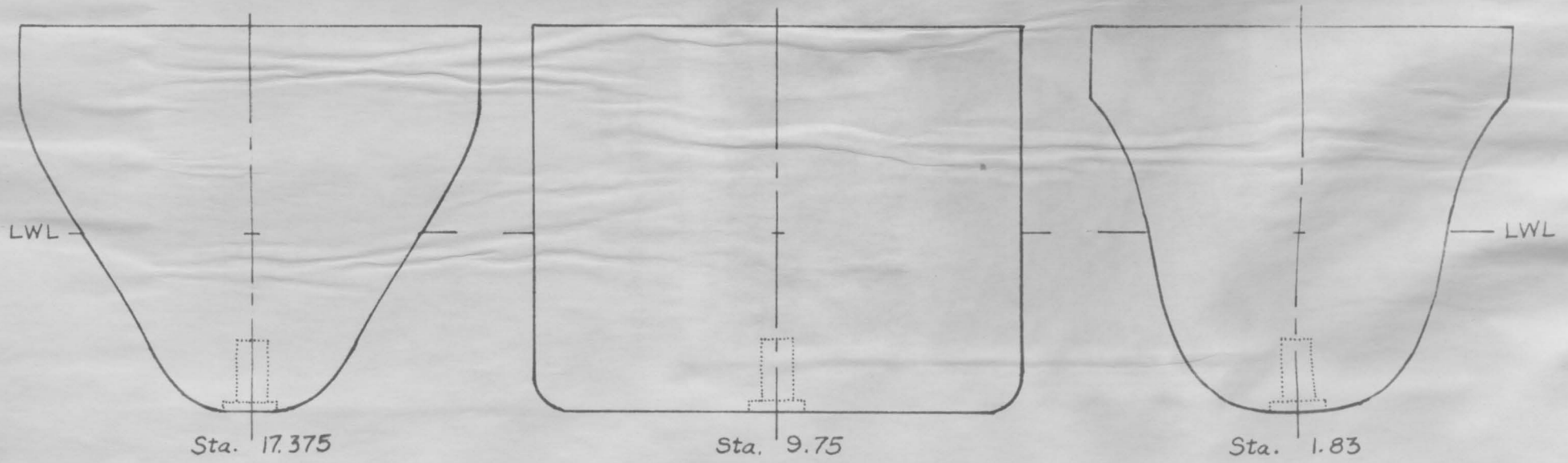

Hull Sections at Gage Locations

MODEL PROFILE AND SECTIONS

Fig. 4

Fig. 5 View of the bottom of the model, showing the location of the pressure gages.

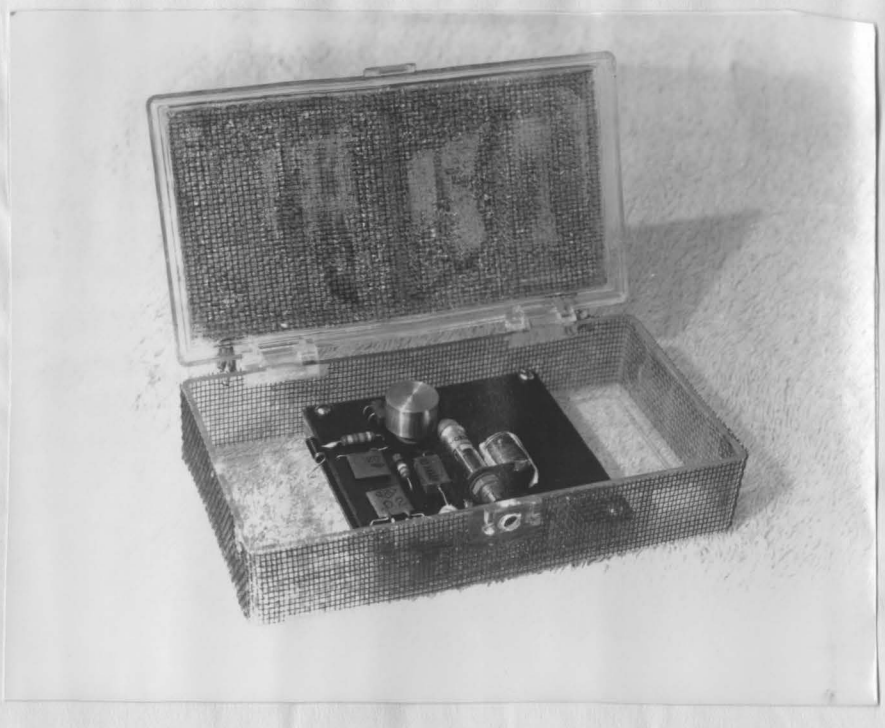

Fig. 6 Capacitance probe transmitter unit before encapsulation. The two-inch square plate is located under the transmitter. Tuning is accomplished by turning the adjustment screw of the small piston capacitor through the hole in the front of the case.

Fig. 7 Capacitance probe transmitter after encapsulation. A brass heat-sink is mounted over the transistor. The battery is externally mounted being connected to the wires at the left.

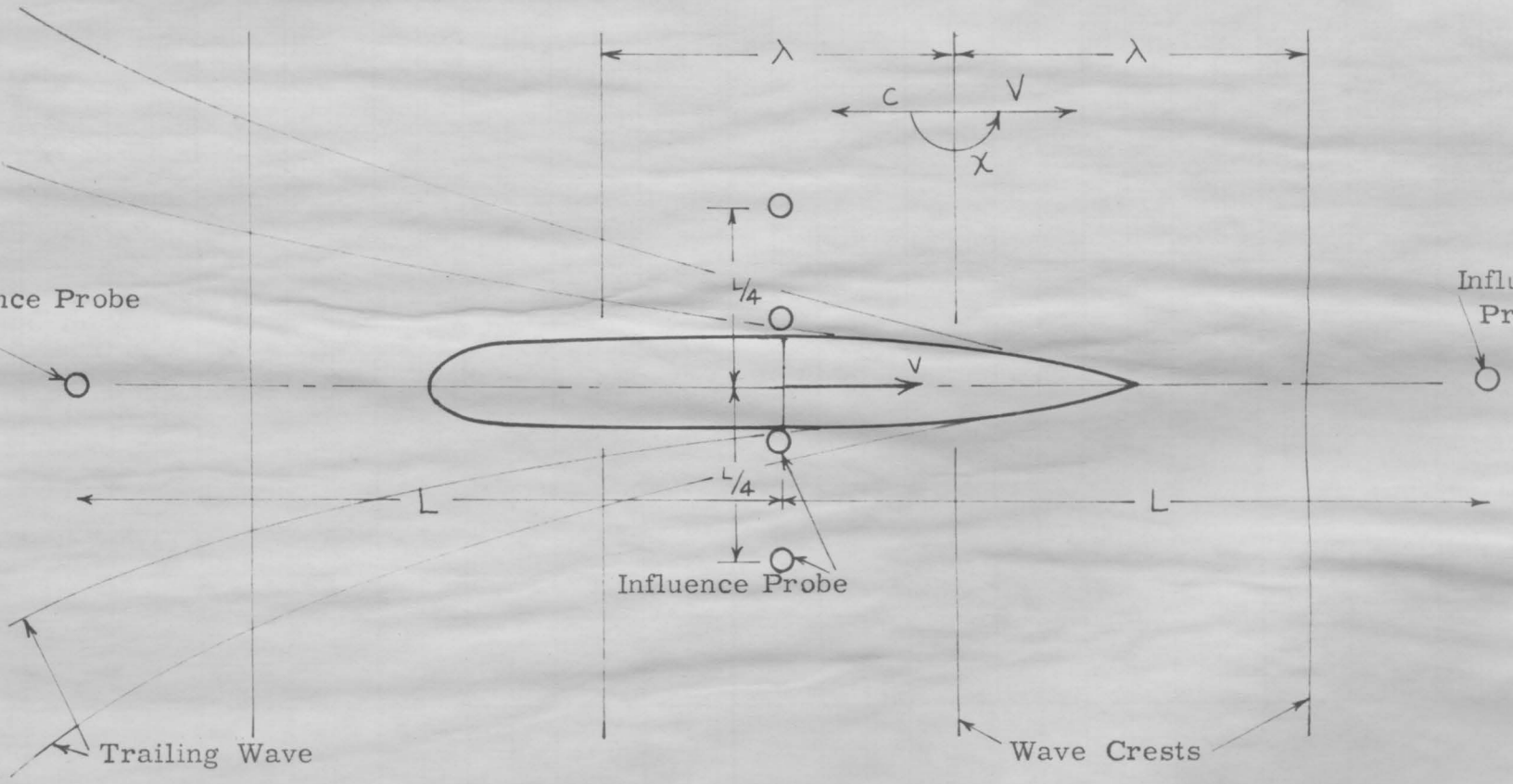

LOCATION OF PROBES IN RELATION TO MODEL AND SEAWAY

Fig. 8

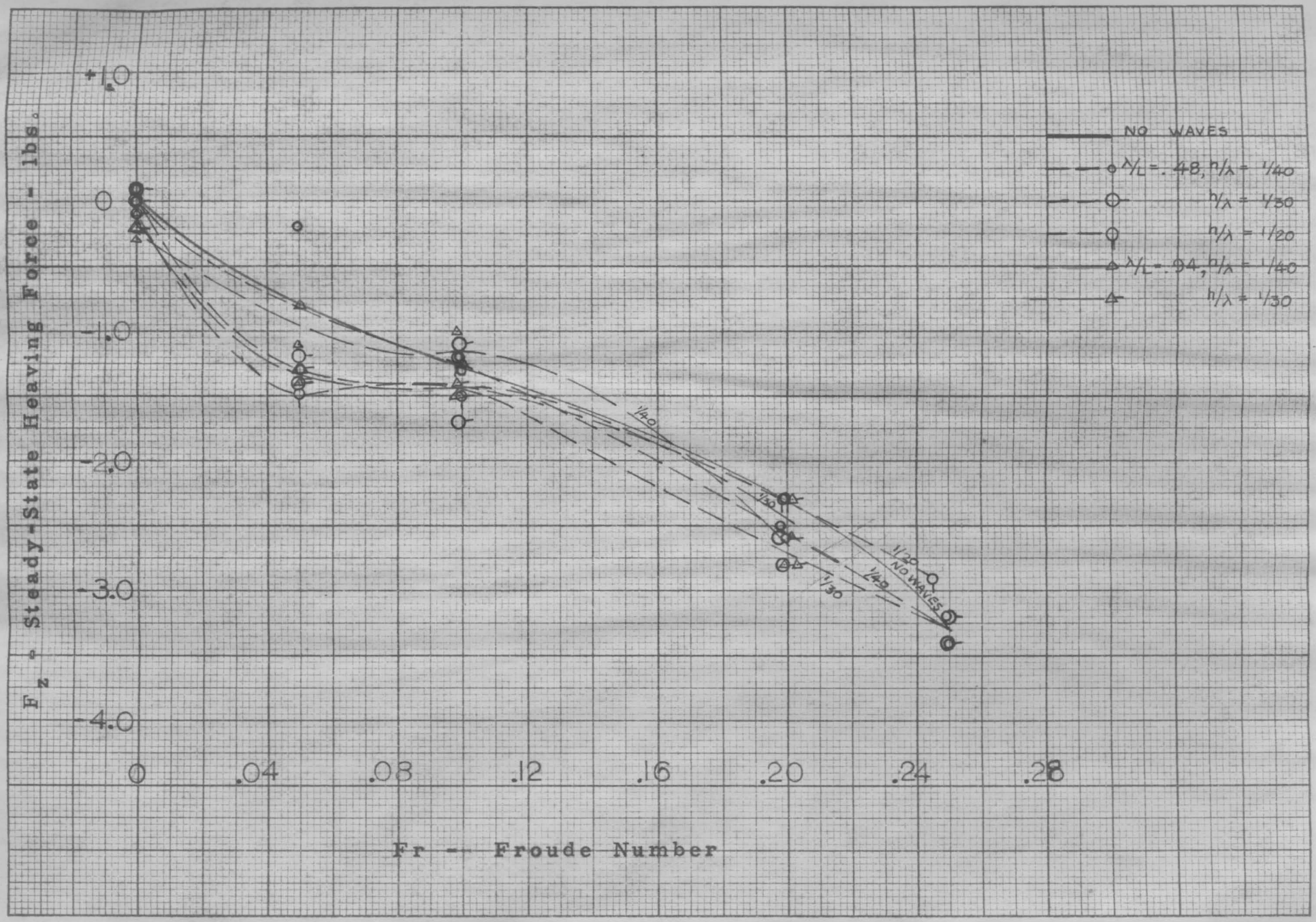

STEADY - STATE HEAVING FORCE

Fig. 9

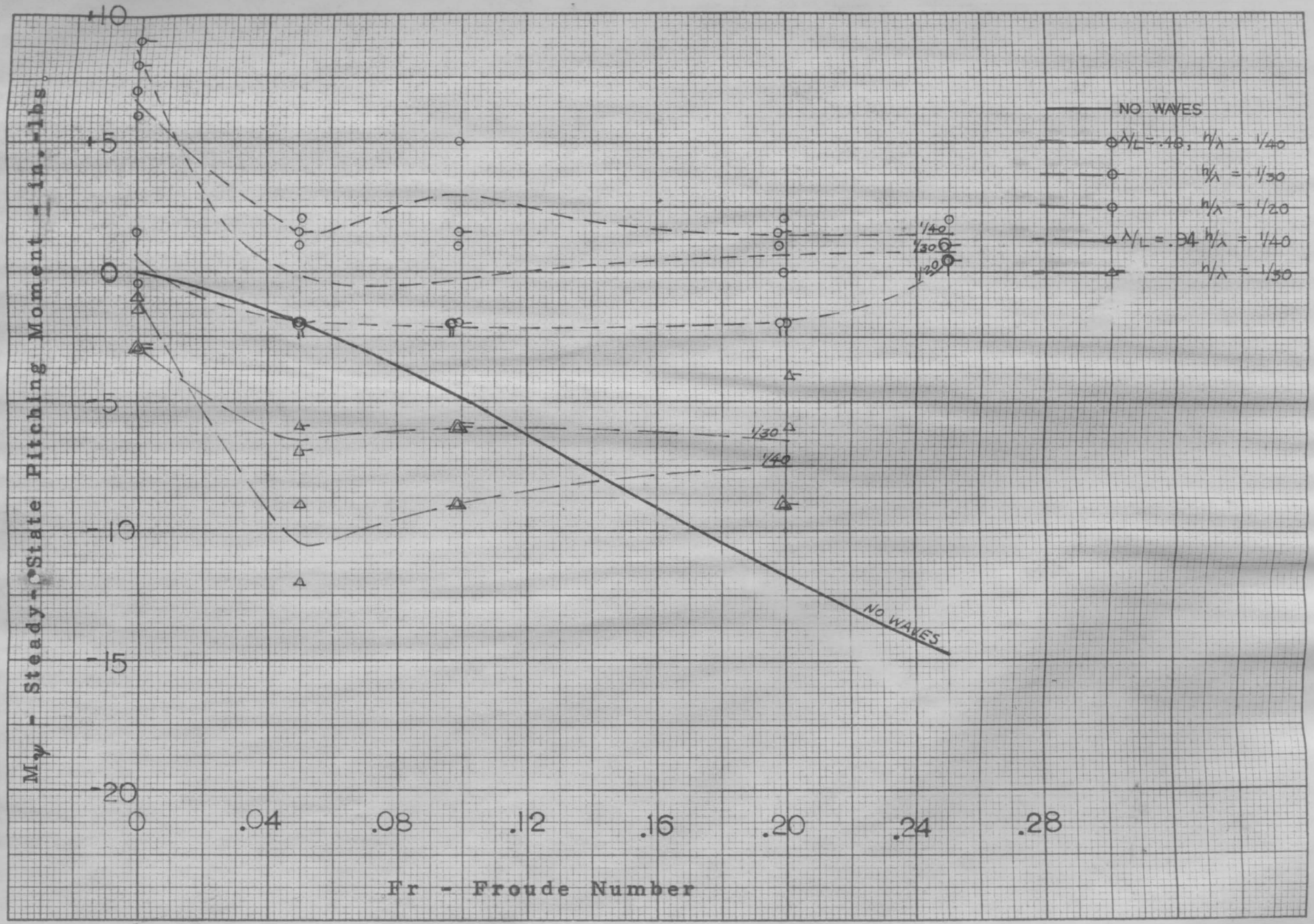

STEADY - STATE PITCHING MOMENT

Fig. 10

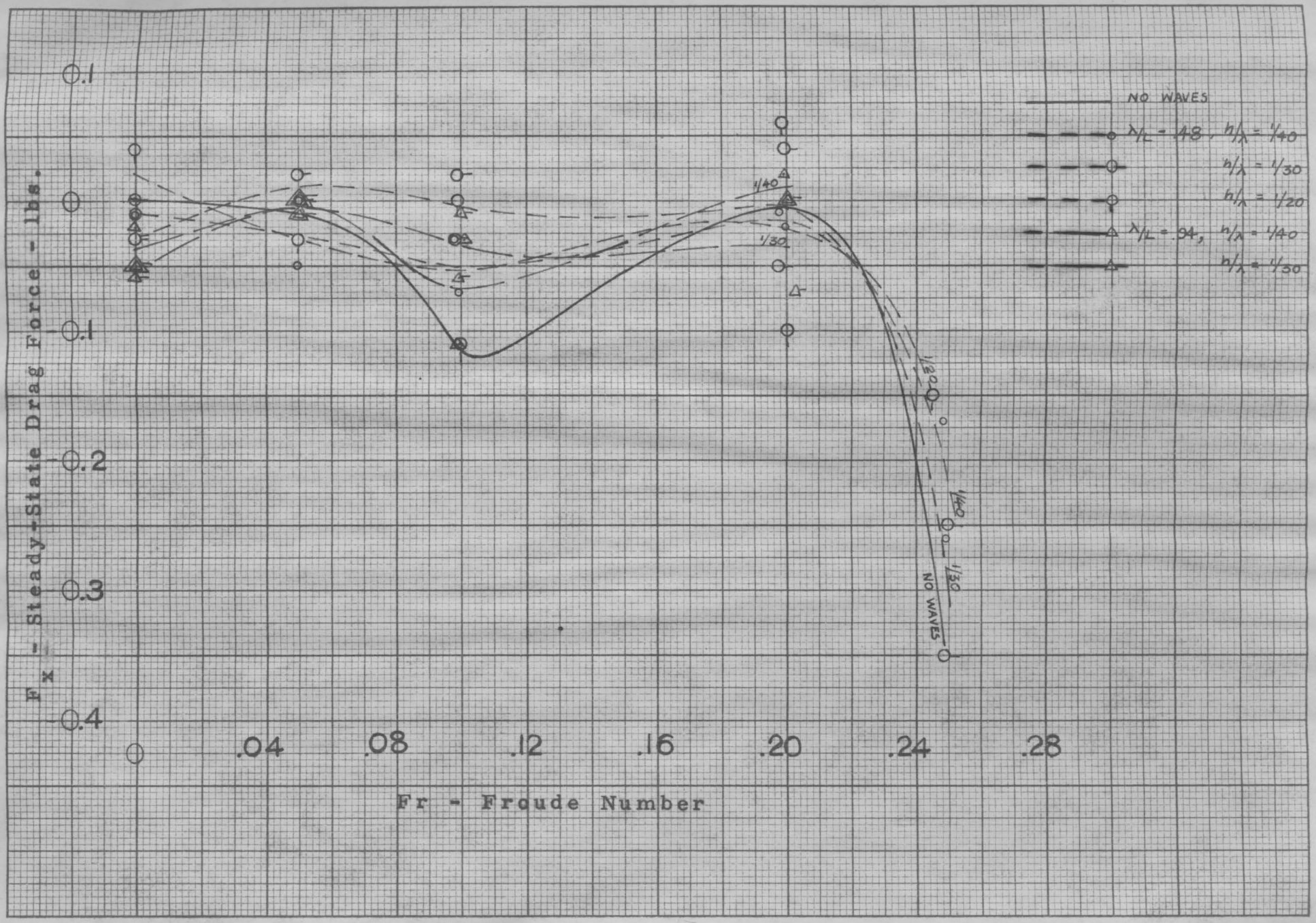

STEADY - STATE DRAG FORCE

Fig. 11

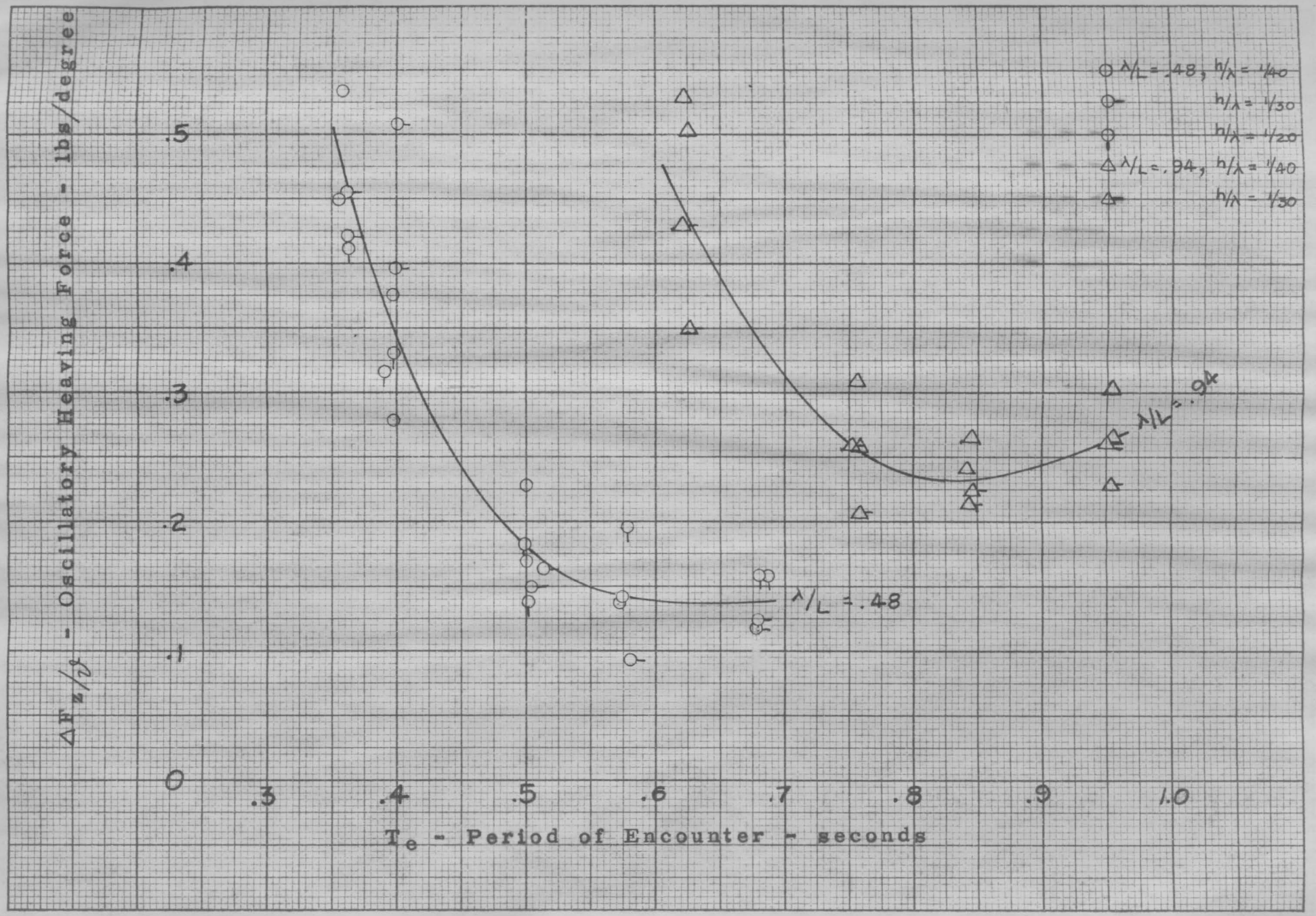

OSCILLATORY HEAVING FORCE

Fig. 12

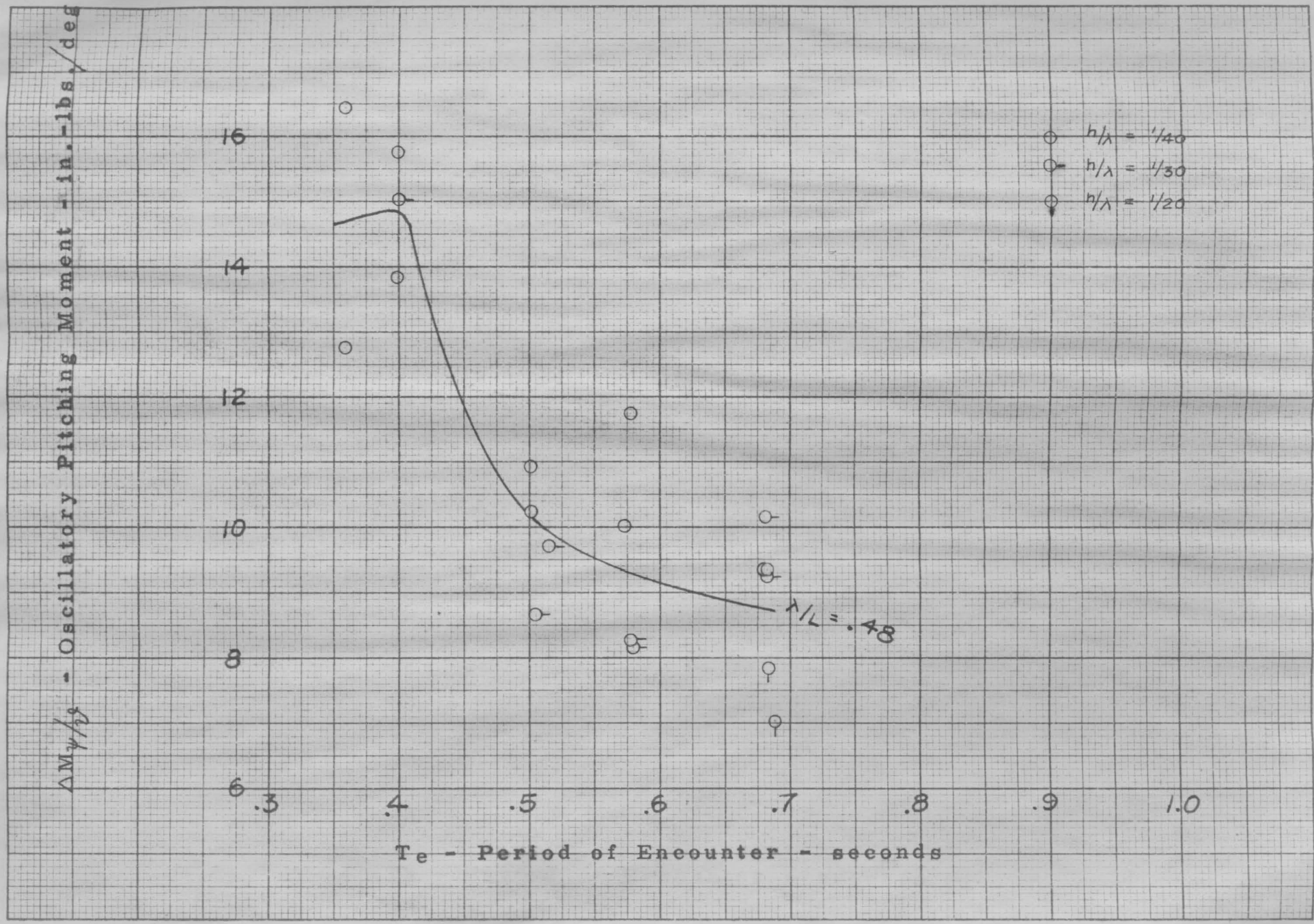

OSCILLATORY PITCHING MOMENT

Fig. 13

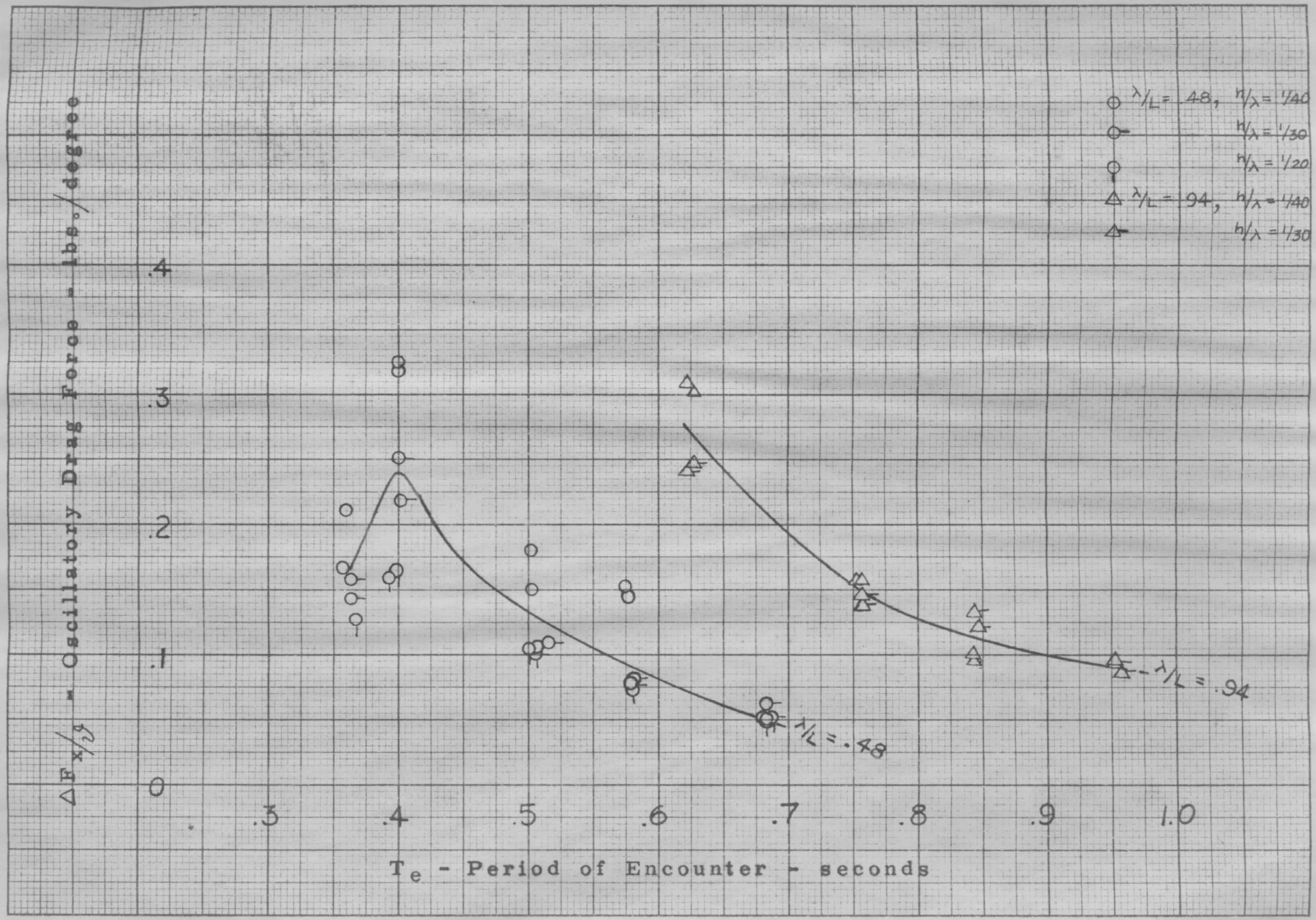

OSCILLATORY DRAG FORCE

Fig. 14

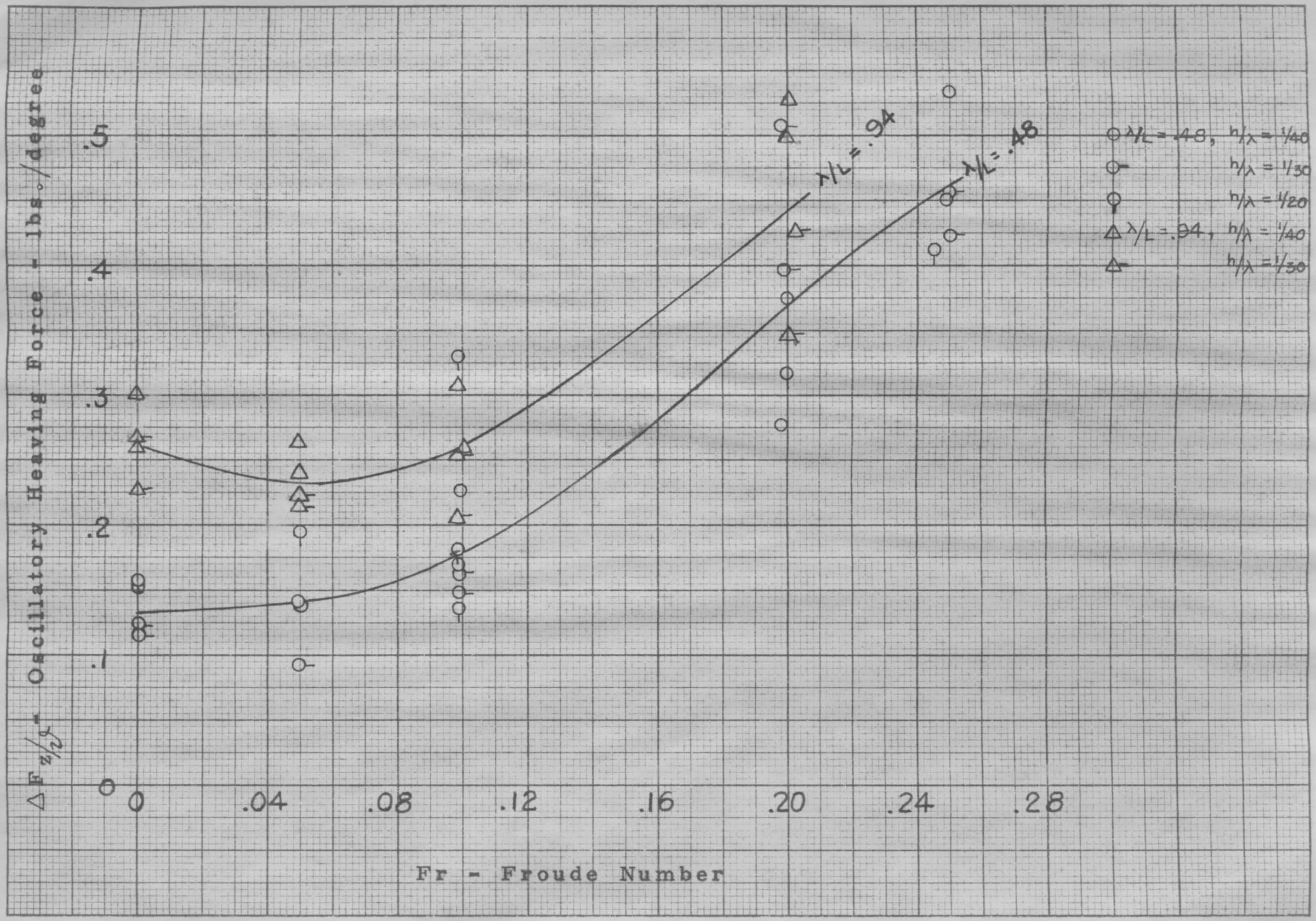

OSCILLATORY HEAVING FORCE

Fig. 15

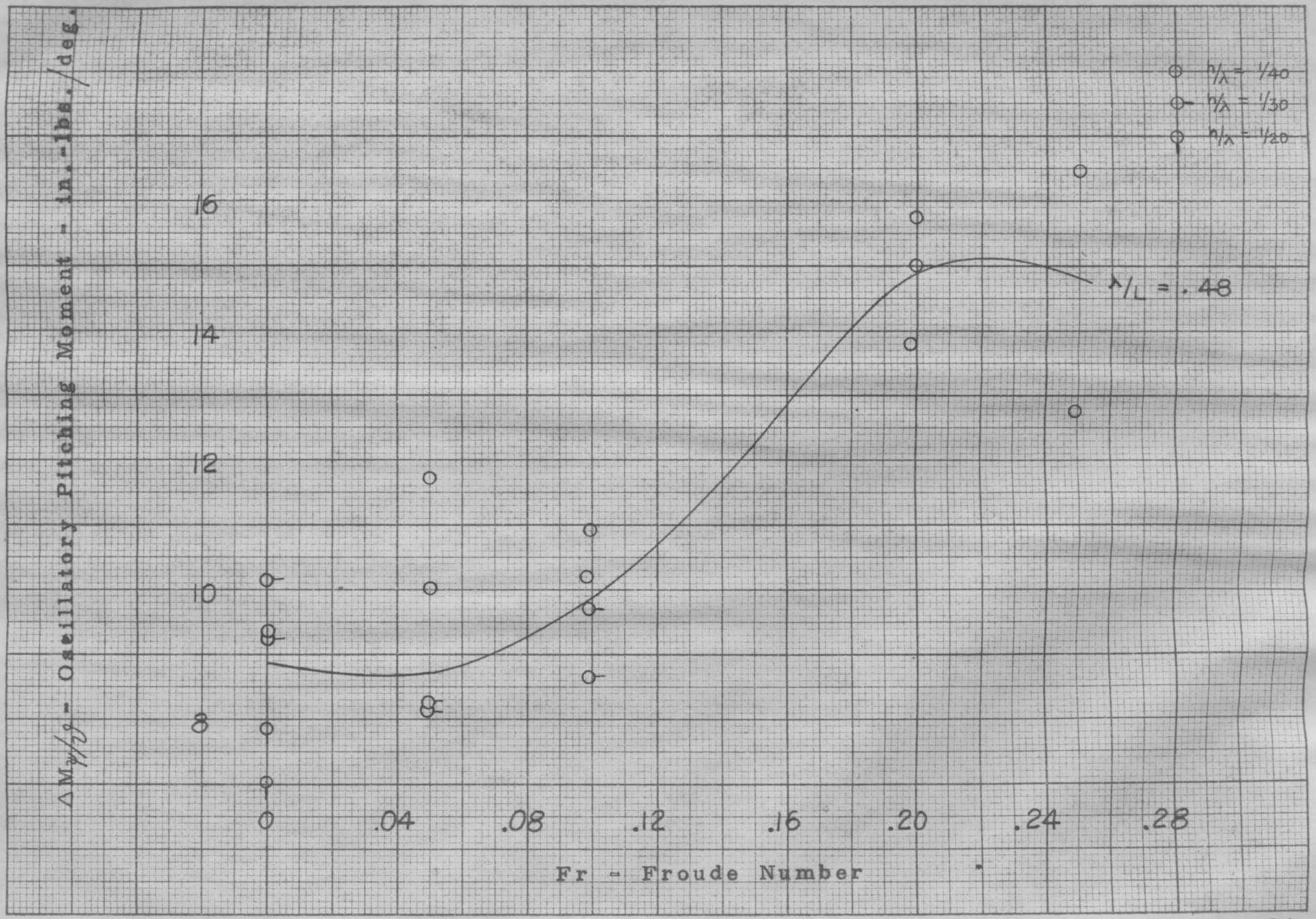

OSCILLATORY PITCHING MOMENT

Fig. 16

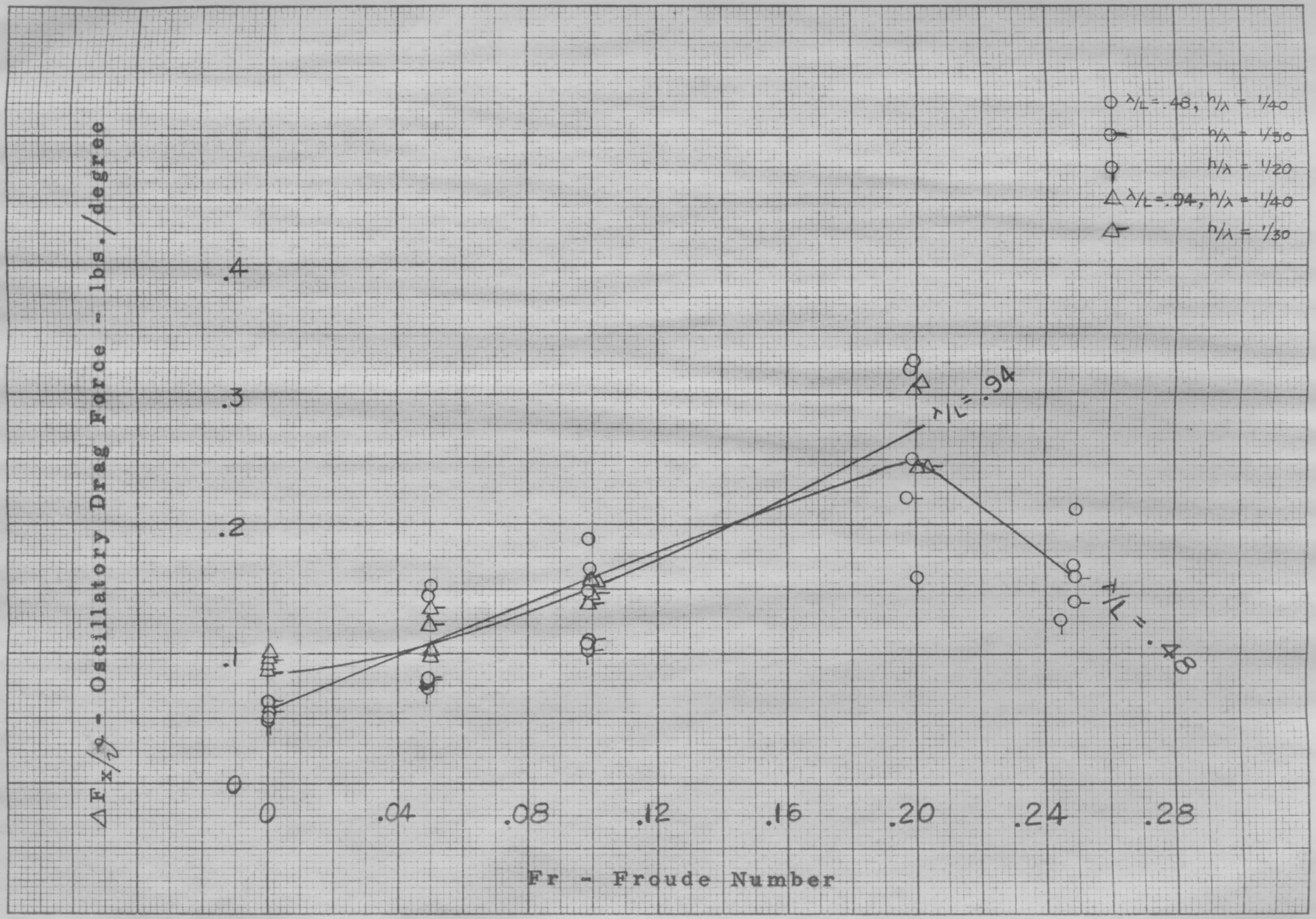

OSCILLATORY DRAG FORCE

Fig. 17

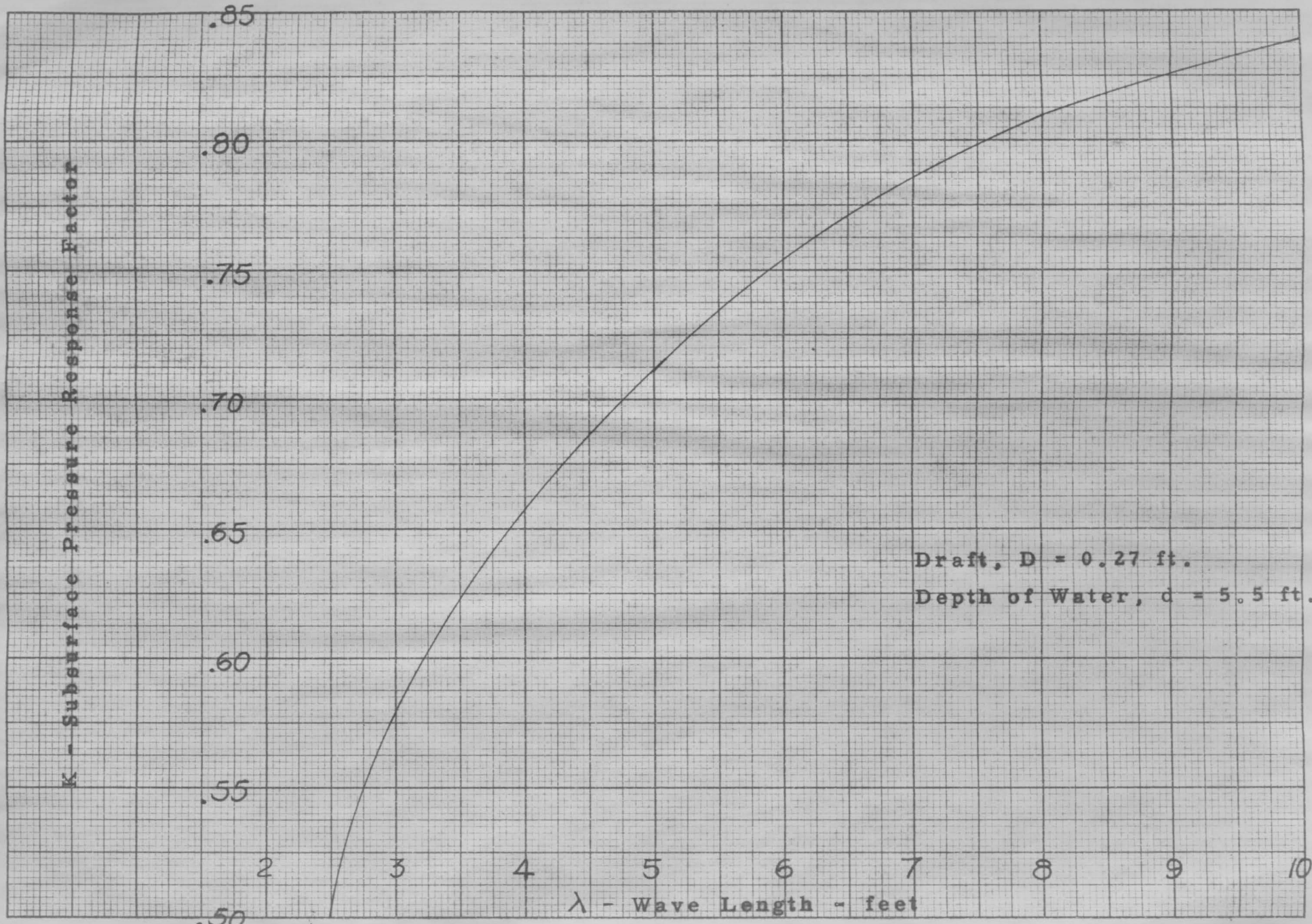

PRESSURE RESPONSE FACTOR FOR BOTTOM OF MODEL Fig. 18

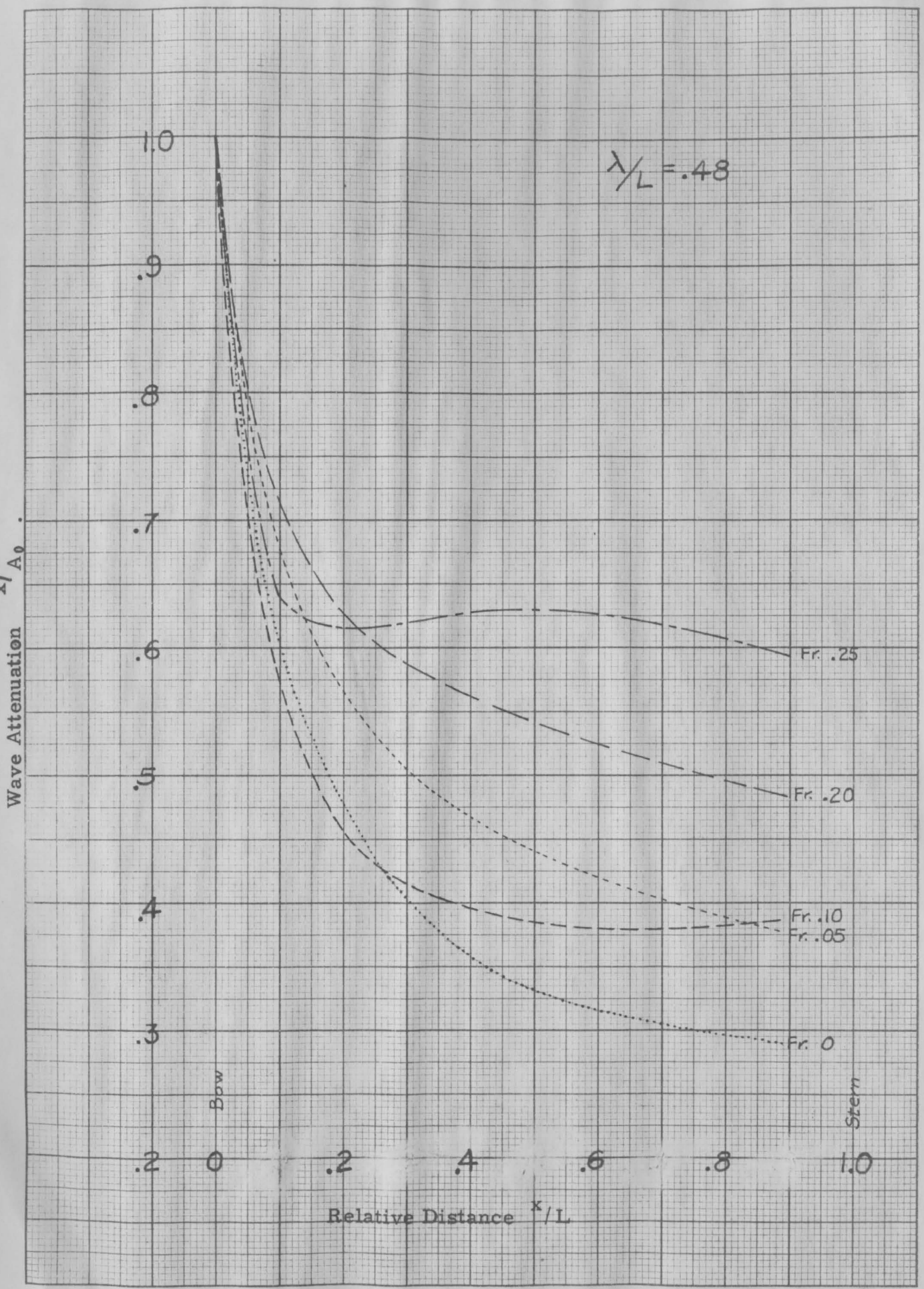

WAVE ATTENUATION AS A FUNCTION OF LENGTH -33- Fig. 19

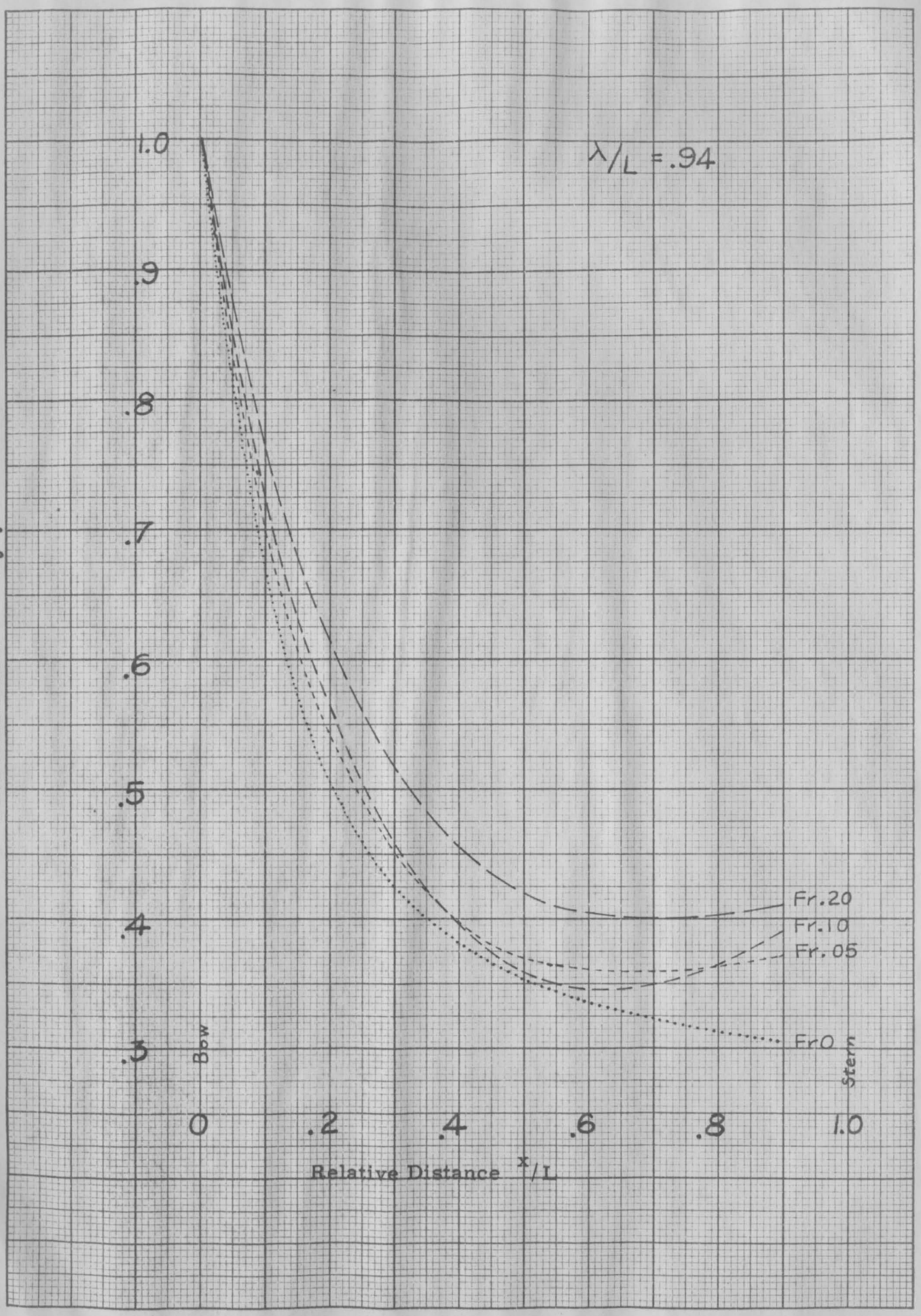

WAVE ATTENUATION AS A FUNCTION OF LENGTH -34- Fig. 20